

# Phase assembly and microstructure of CeO<sub>2</sub>-doped ZrO<sub>2</sub> ceramics prepared by spark plasma sintering

Tao Xu<sup>a</sup>, Peiling Wang<sup>a,\*</sup>, Pingan Fang<sup>a</sup>, Yanmei Kan<sup>a</sup>, Lidong Chen<sup>a</sup>,  
Jef Vleugels<sup>b</sup>, Omer Van der Biest<sup>b</sup>, Jef Van Landuyt<sup>c</sup>

<sup>a</sup> State Key Lab of High Performance Ceramics and Superfine Microstructure, Shanghai Institute of Ceramics, Chinese Academy of Sciences, 200050 Shanghai, China

<sup>b</sup> Department of Metallurgy and Materials Engineering, Katholieke Universiteit Leuven, B-3001 Leuven, Belgium

<sup>c</sup> EMAT, Universiteit Antwerpen, B-2020 Antwerpen, Belgium

Received 21 April 2004; received in revised form 23 August 2004; accepted 27 August 2004

## Abstract

CeO<sub>2</sub>-doped ZrO<sub>2</sub> (8 mol%) starting powder was sintered by means of spark plasma sintering (SPS) at 1300 °C without holding time. The stability of the tetragonal ZrO<sub>2</sub> phase in the Ce-ZrO<sub>2</sub> ceramic sintered under strongly reducing conditions was investigated. The SPS sample consisted of monoclinic and tetragonal ZrO<sub>2</sub> phases with a volume ratio of two to one, as well as a trace amount of a Zr–Ce–O cubic solid solution phase. In contrast, the same powder sintered by hot-pressing in nitrogen at 1300 and 1500 °C for 1 h showed no tetragonal ZrO<sub>2</sub>. Microstructural observation of the SPS ceramic by SEM and TEM revealed grains with and without twins. The reason for the appearance of the tetragonal phase in the SPS sample sintered under strongly reducing conditions is discussed.

© 2004 Elsevier Ltd. All rights reserved.

**Keywords:** Ce-TZP; Spark plasma sintering; Hot-pressing; Phase stability; Microstructure; ZrO<sub>2</sub>

## 1. Introduction

It is well known that ceria-doped zirconia polycrystals (Ce-TZP) exhibit a remarkably high transformation toughness, even when compared to Y-TZP ceramics, and that they are of considerable interest for advanced structural applications.<sup>1–4</sup> However, Ce-TZP is rarely used as a monolithic ceramic due to its relatively low hardness and strength.

Another problem that limits the application of Ce-TZP is the susceptibility to reduction. Reduction of Ce<sup>4+</sup> to Ce<sup>3+</sup> in Ce-TZP ceramics sintered in non-oxidizing atmosphere can be easily observed by the accompanying color change of the sample.<sup>5–9</sup> Even when sintered in air, the central part of a large component will change color, turning orange to brown or even black, depending on the oxygen partial pressure.<sup>5</sup>

Due to the increase in the ionic radius of the cerium ions from 0.101 nm for Ce<sup>4+</sup> to 0.111 nm for Ce<sup>3+</sup>, there is an approximately 40% mismatch in ionic radius with Zr<sup>4+</sup>, resulting in high elastic lattice strain and the segregation of Ce<sup>3+</sup> to the grain boundaries,<sup>10</sup> which causes the destabilization of the tetragonal ZrO<sub>2</sub> phase and concomitant cracking of bulk materials. Heussner and Claussen<sup>7</sup> reported that sintering of Ce-TZP in nitrogen or even hot isostatic pressing of pre-sintered materials in a reducing environment using graphite heating elements is impossible, since the tetragonal phase will be completely destabilized and transformed to monoclinic ZrO<sub>2</sub> during cooling.

Spark plasma sintering (SPS) is a relatively new sintering technique for the rapid consolidation of a variety of ceramic materials, which enables samples to reach the sintering temperature very rapidly. The versatility of SPS allows very quick densification to near theoretical density in a number of metallic, ceramic and multi-layered materials in a low vacuum en-

\* Corresponding author. Tel.: +86 21 52412324; fax: +86 21 52413122.  
E-mail address: [plwang@sunm.shenc.ac.cn](mailto:plwang@sunm.shenc.ac.cn) (P. Wang).

vironment ( $\sim 5$  Pa).<sup>11–13</sup> In the SPS process, a graphite die is filled with the raw material powder, and placed between lower and upper graphite punch electrodes. A mechanical pressure and pulsed direct current (dc) is applied to the sintering powder compact, and the activation of powder particles is achieved by the application of electrical discharges. Typical sintering time can be reduced from several hours for conventional sintering, using an electrical resistance furnace, to approximately 30 min or even less by SPS.

During SPS, there is a strongly reducing atmosphere around the starting powder because graphite is used as die material, so it is reasonable to assume that reduction in CeO<sub>2</sub>-doped ZrO<sub>2</sub> will occur and that no tetragonal phase will be retained at room temperature. To the best of the authors' knowledge, no details of the phase stability and microstructure of Ce-doped ZrO<sub>2</sub> ceramics prepared by SPS have been reported.

In order to investigate whether it is possible to limit or even avoid the reduction by a very short thermal sintering cycle, 8 mol% CeO<sub>2</sub>-doped zirconia powder is densified by spark plasma sintering in the present work. The same powder was sintered by hot-pressing for comparison. The phase stability and microstructure of the 8 mol% Ce-ZrO<sub>2</sub> ceramics sintered under strongly reducing conditions are investigated and discussed.

## 2. Experimental procedure

The starting materials used in the present work are CeO<sub>2</sub> (Yuelong chemicals, Shanghai, China, >99.9%) and ZrO<sub>2</sub> (Yuelong chemicals, Shanghai, China, >99.9%). The mixture of starting materials was ball-milled in a polyethylene jar with zirconia milling balls in ethanol for 24 h, and subsequently dried and sieved through a 100-mesh nylon sieve.

For SPS, the dried powder was inserted into a cylindrical graphite die with a diameter of 20 mm and sintered in a SPS furnace (SPS-2040, Sumitomo Coal Mining Co., Japan) under a uniaxial pressure of 50 MPa in vacuum at 1300 °C without holding time. The heating rate was 150 °C/min. For hot-pressing, the powder was inserted into a graphite die with diameter 20 mm and coated with boron nitride, and hot-pressed in a graphite resistance furnace under a nitrogen flow of 1 atm under a mechanical load of 20 MPa. Hot-pressing was performed at 1300 °C and at 1500 °C for 1 h, respectively. The furnace was cooled by switching off the power.

The density of the sintered bodies was determined using the Archimedes method. The phase composition was characterized by X-ray diffraction using a Guinier-Hägg camera (XDC 1000, Sweden) with Cu K $\alpha$  radiation ( $\lambda = 1.5405981$  Å) and Si as an internal standard. The X-ray film analysis was completed by a computer-linked line scanner (LS-18) system and SCANPI program.<sup>14</sup> The lattice parameters of the tetragonal phase in the SPS material were determined by means of the PIRUM program.<sup>15</sup> The amount of monoclinic phase was estimated using Toyara's

method.<sup>16</sup> Microstructural investigation was performed by scanning electron microscopy (SEM, XL-30FEG, FEI, Eindhoven, The Netherlands) and transmission electron microscopy (TEM, JEOL-2010 and JEOL-4000EX, Japan).

## 3. Results and discussion

Table 1 summarizes the sintering data for the samples prepared in this study, together with the density and constituent phases of the sintered samples. Although the density of the hot-pressed samples increases with increasing sintering temperature in the range of 1300–1500 °C, no fully dense materials can be obtained (see Table 1), whereas a relatively high density of 5.97 g/cm<sup>3</sup> was reached for the SPS sample prepared at 1300 °C without holding time.

The hot-pressed samples cracked completely. Besides, reduction phenomena could be observed easily by the accompanying dark grey color of the samples. The X-ray diffraction patterns in the  $2\theta$  range from 27° to 33° for the samples sintered under different conditions are presented in Fig. 1. It is noted that no trace of tetragonal phase was detected, whereas a large amount of monoclinic phase was formed in the hot-pressed samples. A minor but significant amount of an additional phase was also detected in the XRD patterns. According to the XRD data, this additional phase could be identified as a Zr–Ce–O cubic solid solution, whose XRD

Table 1  
Sintering conditions, densities and phase assembly of the sintered samples

Sintering condition	Density (g/cm <sup>3</sup> )	Phase present <sup>a</sup>
1300 °C/20 MPa/1 h (HP)	4.87	Monoclinic/s, C <sub>ss</sub> /mw
1500 °C/20 MPa/1 h (HP)	5.79	Monoclinic/s, C <sub>ss</sub> /mw
1300 °C/50 MPa/0 min (SPS)	5.97	Monoclinic/s, t/m, C <sub>ss</sub> /tr

<sup>a</sup>C<sub>ss</sub>: Zr–Ce–O cubic solid solution; t: tetragonal; s: strong; m: medium; w: weak; tr: trace.

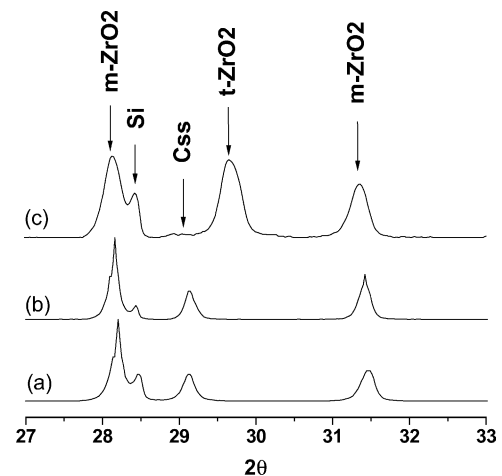


Fig. 1. XRD patterns of the ceramics sintered under different conditions: (a) hot-pressed at 1300 °C, (b) hot-pressed at 1500 °C, and (c) SPS-ed at 1300 °C. The Si was added as internal marker.

pattern was similar to that of  $Zr_{0.4}Ce_{0.6}O_2$  (PDF#38-1439), although the determination of its composition was not carried out.

The influence of different atmospheres on the phase relation of solid solutions in the Zr–Ce–O system has been investigated by Leonov et al.<sup>17,18</sup> They reported that  $Ce^{4+}$  in solid solution of  $ZrO_2$  was reduced to  $Ce^{3+}$  at increased temperatures in reducing atmospheres and in vacuum of  $10^{-1}$  to  $10^{-2}$  Pa. In the present work, the starting powder was prepared by mixing of monoclinic  $ZrO_2$  and pure  $CeO_2$  powder. For the hot-pressing process, the powder was inserted into a graphite die and then hot-pressed in a graphite resistance furnace in nitrogen for 1 h, yielding a strongly reducing environment around the powder during the whole process. Under these conditions, the reduction of  $Ce^{4+}$  ions to  $Ce^{3+}$  will occur. In the present work, there are two possible mechanisms for the reduction of  $Ce^{4+}$  to  $Ce^{3+}$ : (1) during hot-pressing cycle,  $Ce^{4+}$  ions at first enter into  $ZrO_2$  lattice, i.e. interact with  $ZrO_2$ , and then are reduced to  $Ce^{3+}$ , (2) during hot-pressing cycle,  $Ce^{4+}$  ions are reduced to  $Ce^{3+}$  before interaction with  $ZrO_2$ , and it is not known which one is dominant. However, due to the strongly reducing environment and the very low oxygen partial pressure, it is reasonable to consider that all  $Ce^{4+}$  ions will be reduced to  $Ce^{3+}$ .

When all  $Ce^{4+}$  ions are reduced to  $Ce^{3+}$ , relevant phase diagram is the  $ZrO_2$ – $Ce_2O_3$  system<sup>17</sup> as shown in Fig. 2. According to this phase diagram, a cubic  $Ce_2Zr_2O_7$  compound with a pyrochlore (p) structure is in equilibrium with a m- $ZrO_2$ – $CeO_{1.5}$  solid solution or tetragonal solid solution, below and above 1000 °C, respectively, for the composition containing 3–44 mol%  $CeO_{1.5}$ . In the hot-pressed samples, however, no pyrochlore phase but a cubic Zr–Ce–O solid solution was formed instead. This fact can be explained that the hot-pressing cycle in the present work is much shorter than that used for investigation of phase equilibrium, so that the time at elevated temperature might not be enough for this

ternary system to reach complete equilibrium to form the pyrochlore phase during cooling.

The sample sintered by SPS was accompanied by a color change to dark brown, indicating that reduction occurred during sintering. No macrocrack or microcrack formation, however, was observed on the surface of the SPS sample. XRD results indicated the formation of three phases, of which the major crystalline phase is monoclinic  $ZrO_2$ . The minor phase is tetragonal  $ZrO_2$ . The unit cell dimensions of the tetragonal phase are  $a = 5.201$  Å and  $c = 5.233$  Å, indicating an expansion of the  $a$ -axis and a little shrinkage of the  $c$ -axis compared to those of the pure tetragonal  $ZrO_2$  phase ( $a = 5.12$  Å,  $c = 5.25$  Å, PDF#17-0923). This implies that Ce ions entered the  $ZrO_2$  lattice to stabilize the tetragonal phase. The amount of monoclinic and tetragonal phase in the SPS sample, calculated from the XRD data, is 66 and 34 vol.%, respectively. Beside t- and m- $ZrO_2$ , a trace amount of a Zr–Ce–O cubic solid solution was detected.

During SPS, graphite was also used as die and punch material, assuring a strong reducing environment around the sintering powder implying that the reduction of  $Ce^{4+}$  ions would be likely. It was, therefore, interesting to see that only a trace amount of the Zr–Ce–O cubic solid solution was formed and that the tetragonal  $ZrO_2$  could be partially retained at room temperature, which was not the case in the hot pressed ceramics.

Due to the complete sample degradation, microstructural observation on the hot-pressed samples was difficult, and therefore, not carried out. SEM micrographs of the 8 mol%  $CeO_2$  stabilized  $ZrO_2$  SPS sample, which was polished and thermally etched (30 min in air at 1300 °C) before observation, is shown in Fig. 3. Many grains show a regular stripe pattern with intervals ranging from 50 to 150 nm. Because of the very limited amount, it was not possible to find the Zr–Ce–O cubic solid solution by SEM observation.

To further investigate the microstructure of the SPS sample, TEM was performed, revealing the typical and charac-

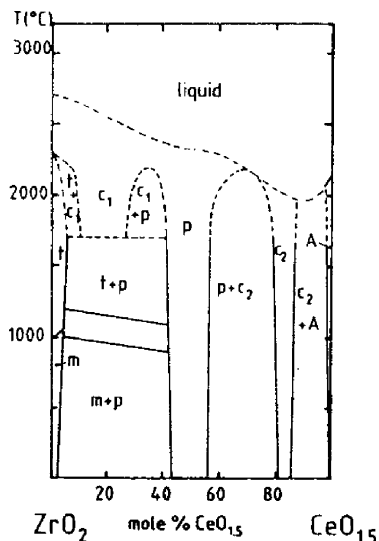


Fig. 2. Phase diagram of the  $ZrO_2$ – $CeO_{1.5}$  system.<sup>17</sup>

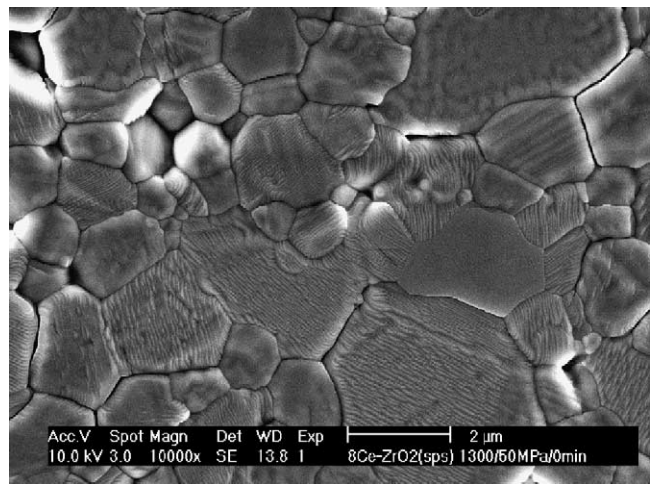


Fig. 3. SEM micrograph of the 8 mol%  $CeO_2$  stabilized  $ZrO_2$  ceramic sintered by SPS.



Fig. 4. TEM micrograph of the 8 mol% CeO<sub>2</sub> stabilized ZrO<sub>2</sub> ceramic sintered by SPS.

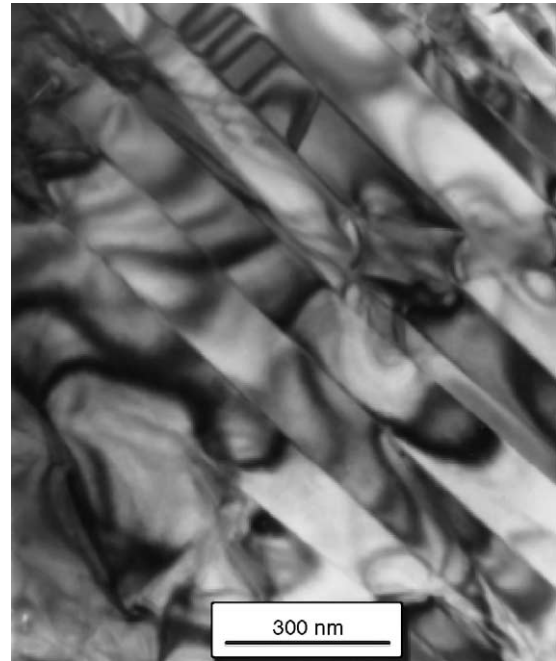


Fig. 5. Detail of a monoclinic grain of the 8 mol% CeO<sub>2</sub> stabilized ZrO<sub>2</sub> ceramic sintered by SPS.

teristic twin pattern of monoclinic ZrO<sub>2</sub> grains, as shown in Figs. 4 and 5. The twinning structure of the monoclinic phase is the product of the athermal martensitic transformation of the tetragonal to monoclinic ZrO<sub>2</sub> phase. This kind of morphology is similar to that which results from the stress-induced tetragonal to monoclinic transformation in Ce-TZP reported in the literature.<sup>19,20</sup> It is, therefore, not excluded that a fraction of tetragonal grains transformed during TEM sample preparation. Although a large amount of monoclinic grains were observed on the polished surface, only a limited extent of microcracking could be found, which indicates the good self-accommodation between the grains.

Energy dispersive point analyses were obtained during TEM analysis, as illustrated in Fig. 6. The analysis results of the indicated points are summarized in Table 2. The EDS spectra of grains with a different morphology proved that the monoclinic ZrO<sub>2</sub> grains with twinning structure contain less Ce (<2 mol%) than the tetragonal grains without twinning structure (~10 mol%). According to the EDS results

summarized in Table 2, assuming that the Zr ions retain the tetravalent state and the O<sup>2-</sup> content for Zr<sup>4+</sup> is subtracted from the total amount of measured O ions, the remaining O<sup>2-</sup> content is not enough to keep the Ce ions in the tetravalent state. On the other hand, the O/Ce ratio is about 1.5/1 in both the monoclinic and tetragonal grains, supporting the view that all Ce<sup>4+</sup> ions are reduced to Ce<sup>3+</sup> during SPS sintering.

Despite the complete reduction of Ce<sup>4+</sup> to Ce<sup>3+</sup>, the tetragonal phase could be partially retained at room temperature in the SPS sample. On the other hand, only a trace amount of a Zr–Ce–O cubic solid solution was formed, clearly different from the phase assembly of the hot-pressed samples. The results of EDS analysis and unit cell dimensions of the SPS sample revealed the tetragonal ZrO<sub>2</sub> phase stabilizing effect of Ce<sup>3+</sup>. Although it is understood that the stabilization of t-ZrO<sub>2</sub> by Ce<sup>3+</sup> is difficult, due to the approximately 40% mismatch in ionic radii of Ce<sup>3+</sup> with Zr<sup>4+</sup> resulting in high elastic lattice strain,<sup>10</sup> the present results indicate it is possible using a very rapid SPS sintering cycle. The exact mechanism, however, remains unclear.

Table 2  
EDS results of different point analysis at the locations indicated in Fig. 6

Point no.	Zr (at.%)	Ce (at.%)	O (at.%)	O for Zr <sup>a</sup> (at.%)	O for Ce (at.%)	O/Ce ratio	ZrO <sub>2</sub> (mol%)
1	30.40	3.52	66.08	60.80	5.28	1.50	89.62
2	32.84	0.60	66.57	65.68	0.89	1.48	98.20
3	32.94	0.47	66.59	65.88	0.71	1.51	98.59
4	33.01	0.39	66.60	66.02	0.58	1.49	98.83
5	32.98	0.42	66.60	65.96	0.64	1.52	98.74

<sup>a</sup>Zr ions are assumed to retain their tetravalent state.



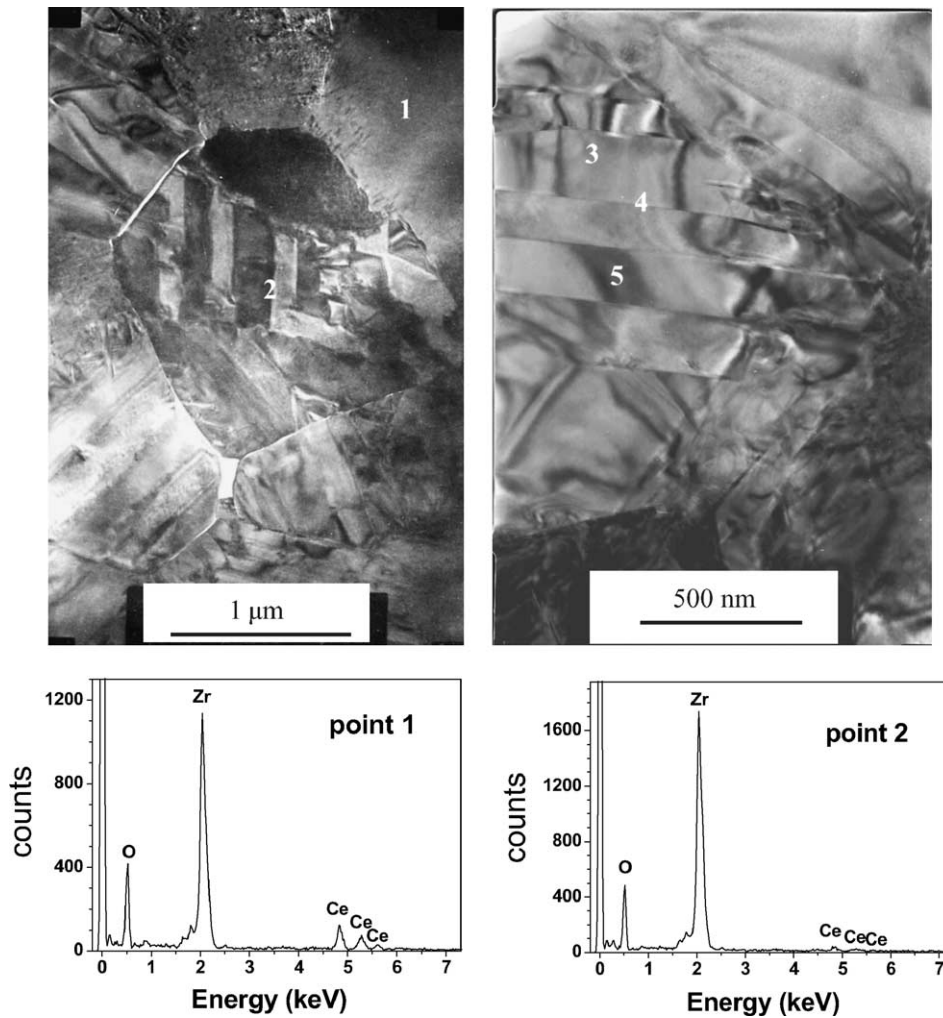


Fig. 6. TEM micrographs and EDS spectra taken from different grains in the 8 mol%  $\text{CeO}_2$  stabilized ceramic sintered by SPS. The analysis results of the labelled positions are summarized in Table 2.

#### 4. Conclusions

Fully densified 8 mol%  $\text{CeO}_2$ -doped zirconia was obtained by means of spark plasma sintering (SPS) at  $1300^\circ\text{C}$  without holding time. Although the powder was sintered under strongly reducing conditions and complete reduction of  $\text{Ce}^{4+}$  to  $\text{Ce}^{3+}$  occurred, a fraction of tetragonal  $\text{ZrO}_2$  could be retained at room temperature. Besides the t- $\text{ZrO}_2$  phase, a large amount of m- $\text{ZrO}_2$  phase and a trace amount of a Zr–Ce–O cubic solid solution were observed. In contrast, no t- $\text{ZrO}_2$  could be retained when hot pressing for 1 h at 1300 and  $1500^\circ\text{C}$ , whereas a significant amount of the Zr–Ce–O cubic solid solution was observed.

#### Acknowledgements

This work is financially supported by the Flanders–China bilateral projects (BIL 02/06). Tao Xu thanks Mr. Shengqiang Bai for the operation of the spark plasma sintering system.

#### References

1. Tsukuma, K., Mechanical properties and thermal stability of  $\text{CeO}_2$  containing tetragonal zirconia polycrystals. *Am. Ceram. Soc. Bull.*, 1986, **65**, 1386–1389.
2. Tsukuma, K. and Shimada, M., Strength, fracture toughness, and vickers hardness of Ce-stabilized tetragonal zirconia polycrystals (Ce-TZP). *J. Mater. Sci.*, 1985, **20**, 1178–1184.
3. Bhaduri, S. B., Chakraborty, A. and Rao, R. M., Method of fabrication ceria-stabilized tetragonal zirconia polycrystals. *J. Am. Ceram. Soc.*, 1988, **71**, C-410–C-411.
4. Wang, J., Zheng, X. H. and Stevens, S., Fabrication and microstructure–mechanical property relationships in Ce-TZPs. *J. Mater. Sci.*, 1992, **27**, 5348–5356.
5. Cawley, J. D. and Lee, W. E., Oxide ceramics. In *Materials Science and Technology: Structure and Properties of Ceramics II*, ed. M. Swain. VCH, Weinheim, Germany, 1994, p. 101.
6. Kountouros, P. and Petzow, G., Defect chemistry, phase stability and properties of zirconia polycrystals. In *Science and Technology of Zirconia V*, ed. S. P. S. Badwal, M. J. Bannister and R. H. J. Hannink. Technomic Publishing Co, Lancaster, USA, 1993, pp. 30–48.
7. Heussner, K.-H. and Claussen, N., Strengthening of ceria-doped tetragonal zirconia polycrystals by reduction-induced phase transformation. *J. Am. Ceram. Soc.*, 1989, **72**, 1044–1046.

8. Theunissen, G. S. A. M., Winnubst, A. J. A. and Burggraaf, A. J., Effect of dopants on the sintering behaviour and stability of tetragonal zirconia ceramics. *J. Eur. Ceram. Soc.*, 1992, **9**, 251–263.
9. Shigematsu, T., Shiokawa, N., Machida, N. and Nakanishi, N., Martensitic transformation in deoxidized ceria-zirconia ceramics. In *Science and Technology of Zirconia V*, ed. S. P. S. Badwal, M. J. Bannister and R. H. J. Hannink. Technomic Publishing Co, Lancaster, USA, 1993, pp. 117–124.
10. Hwang, S. L. and Chen, I.-W., Grain size control of tetragonal zirconia polycrystals using the space charge concept. *J. Am. Ceram. Soc.*, 1990, **73**, 3269–3277.
11. Nygren, M. and Shen, Z., On the preparation of bio-, nano- and structural ceramics and composites by spark plasma sintering. *Solid State Sci.*, 2003, **5**, 125–131.
12. Takeuchi, T., Tabuchi, M., Kageyama, H. and Suyama, Y., Preparation of dense BaTiO<sub>3</sub> ceramics with submicrometer grains by spark plasma sintering. *J. Am. Ceram. Soc.*, 1999, **82**, 939–943.
13. Kobayashi, Y., Takeuchi, T., Tabuchi, M., Ado, K. and Kageyama, H., Densification of LiTi<sub>2</sub>(PO<sub>4</sub>)<sub>3</sub>-based solid electrolytes by spark-plasma-sintering. *J. Power Sources*, 1999, **81/82**, 853–858.
14. Johansson, K. E., Palm, T. and Werner, P.-E., An automatic microdensitometer for X-ray powder diffraction photographs. *J. Phys. E: Sci. Instrum.*, 1980, **13**, 1289–1291.
15. Werner, P.-E., A fortran program for least-square refinement of crystal structure cell dimension. *Arkiv. Kemi.*, 1969, **31**, 513–516.
16. Toyara, H., Yoshimura, M. and Shigeyuki, S., Calibration curve for quantitative analysis of the monoclinic-tetragonal ZrO<sub>2</sub> system by X-ray diffraction. *J. Am. Ceram. Soc.*, 1984, **67**, C-119–C-121.
17. Leonov, A. I., Andreeva, A. B. and Keler, E. K., Influence of the gas atmosphere on the reaction of zirconium dioxide with oxides of cerium. *Izv. Akad. Nauk SSSR Neorganicheskie Mater.*, 1966, **2**, 137–144.
18. Leonov, A. I., Keler, E. K. and Andreeva, A. B., Influence of gaseous medium on chemical reactions and polymorphic transformations in the system zirconium dioxide-cerium oxides. *Ogneupory*, 1966, **31**, 42–48.
19. Hugo, G. R. and Muddle, B. C., The tetragonal to monoclinic transformation in ceria-zirconia. *Mater. Sci. Forum.*, 1988, **34–36**, 165–169.
20. Hugo, G. R., Muddle, B. C. and Hannink, R. H. J., Crystallography of the tetragonal to monoclinic transformation in ceria-zirconia. *Mater. Sci. Forum.*, 1990, **56–58**, 357–362.